Theoretical Evidence for a Dense Fluid Precursor to Crystallization

James F. Lutsko and Grégoire Nicolis
Center for Nonlinear Phenomena and Complex Systems, Université Libre de Bruxelles, C.P. 231, Boulevard du Triomphe, 1050 Brussels, Belgium
(Received 29 July 2005; published 2 February 2006)

We present classical density functional theory calculations of the free-energy landscape for fluids below their triple point as a function of density and crystallinity. We find that, both for a model globular protein and for a simple atomic fluid modeled with a Lennard-Jones interaction, it is free-energetically easier to crystallize by passing through a metastable dense fluid in accord with the Ostwald rule of stages but in contrast to the alternative of ordering and densifying at once as assumed in the classical picture of crystallization.

DOI: 10.1103/PhysRevLett.96.046102 PACS numbers: 87.15.Nn, 05.20.Jj, 82.60.Nh

Crystallization is an intricate process of fundamental importance in many areas of physics, chemistry, and engineering. The classical picture of crystallization from supersaturated solutions goes back to Gibbs and consists of the spontaneous formation of crystalline clusters, which then either grow or shrink depending on the relative importance of the free-energy gain due to the lower bulk free energy of the crystal cluster and the free-energy penalty due to the surface tension between the two phases. In this picture, the local density is the only order parameter: The crystalline cluster is (in general) denser than the fluid. In recent years, this picture has been called into question by simulation, theory, and experiment for the particular and important case of the crystallization of globular proteins. ten Wolde and Frenkel (hereafter tWF) showed by means of simulation that the free-energy landscape of protein crystal clusters as a function of the number of atoms in the cluster and the ''crystallinity'' favored paths leading from no clusters to clusters with low order to ordered clusters over paths moving from no clusters directly to ordered clusters [1]. This picture was confirmed by Talanquer and Oxtoby [2] and Shiryayev and Gunton [3], who showed using a parametrized van der Waals-type model of globular proteins that surface wetting did indeed lower the free energy of crystal clusters. More recently, the simple picture has also been challenged by novel experimental investigations. Vekilov and co-workers have shown that, prior to crystallization, protein solutions harbor metastable droplets of dense fluid, and they have suggested that these droplets are necessary precursors of crystallization [4–6]. In this Letter, we show by means of classical density functional theory calculations that there is an *intrinsic* free-energy advantage in first densifying into a metastable dense-fluid state and then crystallizing rather than following the classical path which goes directly from gas to crystal. Furthermore, our calculations suggest that a similar advantage exists for fluids of small molecules, modeled here via the Lennard-Jones (LJ) interaction, thus indicating that this mechanism may underlie *most* crystallization processes.

The starting point for our analysis is classical density functional theory (DFT) which is based on a theorem, due to Mermin, that the Helmholtz free energy of a classical system is a unique functional $F[\rho]$ of the local density $\rho(\vec{r})$. The local density is a constant, $\rho(\vec{r}) = \bar{\rho}$, for a bulk liquid, while for a simple bulk solid it is a sum of localized functions centered on the lattice sites,

$$\rho(\vec{r}) = \sum_{i=0} f(\vec{r} - \vec{R}_i), \tag{1}$$

for some function $f(\vec{r})$, where the vectors $\{\vec{R}_i\}$ are the lattice vectors. Typically, in a bulk solid, this is approximated as a Gaussian, $f(\vec{r}) = \eta_0(\frac{\alpha}{\pi})^{3/2}\exp(-\alpha r^2)$, where $\eta_0 \in [0, 1]$ is the fraction of lattice sites which are occupied and the parameter α is related to the degree of crystallinity. The average density for a lattice with N_0 lattice sites per unit cell is $\bar{\rho} = \frac{1}{V}\int_V \rho(\vec{r})d\vec{r} = \eta_0 N_0 a^{-3}$, where a is the lattice constant and V is the volume of the system. Given the Gaussian approximation, the density can also be written in terms of Fourier components as

$$\rho(\vec{r}) = \bar{\rho} + \bar{\rho}\sum_{i=1} \exp(i\vec{K}_i \cdot \vec{r})\exp(-K_i^2/4\alpha), \tag{2}$$

where $\{\vec{K}_i\}$ are the reciprocal lattice vectors. This form shows clearly that as α goes to zero, the density becomes uniform corresponding to a fluid, whereas the real-space form shows that, as α goes to infinity, the density becomes infinitely localized as a sum of Dirac delta functions. For this reason, it is natural to take $m \equiv \exp(-K_1^2/4\alpha)$ to be an order parameter measuring ''crystallinity,'' since it becomes zero for the liquid and one for the infinitely localized solid. The use of two order parameters, average density $\bar{\rho}$ and crystallinity m, will allow us to explore different pathways from the gas/liquid to the solid. Using two order parameters thus provides a richer space of possible behaviors and intermediate states than does a single order parameter [7]. Note, however, that this is a minimal extension beyond a single order parameter: In general, the solid phase is characterized by many order parameters, but

the Gaussian approximation made here means that the other order parameters can be expressed as functions of these two [8].

In order to use DFT in practical calculations, it is of course necessary to know the functional $F[\rho]$. Good approximations exist for this functional for the special case of hard-sphere interactions, but the extension of these to other potentials has proven difficult. For this reason, liquid- and solid-state perturbation theory are often used as a means of using the hard-sphere theory to approximate the functional for other systems [9]. Indeed, simple manipulations yield the exact relation

$$\beta F[\rho] = \beta F^{\mathrm{HS}}[\rho; d] + \beta \Delta F(\bar{\rho}) - \int_V \int_V [\rho(\vec{r}_1) - \bar{\rho}][\rho(\vec{r}_2) - \bar{\rho}] \times \int_0^1 (1 - \lambda) \Delta c_2(\vec{r}_1, \vec{r}_2; [\rho_\lambda], d[\rho_\lambda]) d\lambda d\vec{r}_2 d\vec{r}_1, \quad (3)$$

where β is the inverse temperature, $F^{\mathrm{HS}}[\rho; d]$ is the free-energy functional for a hard-sphere system with hard-sphere diameter $d[\rho]$, and $\Delta F(\bar{\rho})$ is the difference in free energy of a liquid at density $\bar{\rho}$ and that of a hard-sphere liquid at the same density. In the integral, $\Delta c_2(\vec{r}_1, \vec{r}_2; [\rho_\lambda], d[\rho_\lambda])$ is the difference in 2-body direct correlation functions (DCFs) for the interacting system and the hard-sphere system for a density $\rho_\lambda(\vec{r}) = \bar{\rho} + \lambda[\rho(\vec{r}) - \bar{\rho}]$. The DCFs are not known exactly, and so it is necessary to introduce approximations to proceed. Motivated by the fact that, in applications of thermodynamic perturbation theory to simple fluids, the correction to the hard-sphere free energy is typically similar for fcc solids and liquids, we will make the simplest approximation, which is to assume that the contribution of the third term is insignificant. This model has been shown to work well for the LJ potential [10] while using the more detailed model of Curtin and Ashcroft [9], which is closely tied to the LJ potential, we indeed find the third term to contribute little. More sophisticated approximations will be discussed in a future publication. Here our interest is not the further development of DFT but in its application to the question of the kinetics of crystallization.

In the following, we use the first order Weeks-Chandler-Andersen perturbation theory [11,12] as modified by Ree *et al.* [13] to calculate the free energy of the liquid phase. This theory is known to be very accurate for a wide class of potentials. The liquid-phase hard-sphere diameter calculated from this theory is used for both the liquid and the solid phases, so that it is indeed solely a function of the average density. For the hard-sphere free-energy functional, we use the fundamental measure theory (FMT), specifically the "white bear" functional [14–16], which gives a good description of the hard-sphere phase diagram, in particular, reproducing the Carnahan-Starling equation of state for the hard-sphere liquid. The use of the FMT free-energy model is critical: Previous attempts to perform similar studies made use of effective liquid approximations, which do not work well when the occupancy is treated as a free variable and which, therefore, had to be modified in an *ad hoc* manner [8,17]. The FMT have built into them the critical feature that they are sensitive to the local density and correctly cause the free energy to diverge if the local occupancy grows above one.

The calculations presented here were performed using the standard LJ potential $v_{\mathrm{LJ}}(r) = 4\varepsilon[(\frac{\sigma}{r})^{12} - (\frac{\sigma}{r})^{6}]$, widely used as a model for the interactions of atomic fluids, and the potential of tWF $v_{\mathrm{tWF}}(r)$, which is intended to model the interactions of globular proteins [1]. The latter consists of a hard core of diameter σ and a modified LJ tail $v_{\mathrm{tWF}}(r) = v_{\mathrm{LJ}}[\lambda^{1/6}(r^2 - \sigma^2)^{1/2}]$ for $r > \sigma$, where λ controls the range of the interaction; following Ref. [1], we take $\lambda = 50$. Figure 1 shows the phase diagrams for both interaction models calculated using our simplified DFT. (Note that the DFT also predicts a spinodal line, but, for clarity, it has not been shown.) In both cases, the phase diagrams are reproduced surprisingly well given the simple models used. The observed deviations from the simulation data can be at least partly explained as arising from the use of the liquid-state free-energy difference for the solid, which requires knowledge of the liquid state at high densities for which even the input hard-sphere equation of state is not reliable. Furthermore, the determination of phase coexistence is a very sensitive test, since it depends on getting both the absolute magnitude and the slope of the free energies correct. To put this in perspective, deviations are observed in Fig. 1 between the calculated and simulated gas-liquid coexistence curve for the LJ system even though the liquid-state perturbation theory gives free energies which differ from simulation by less than 1% [13].

The difference between the phase diagrams of the two interaction models is significant and generic. Whereas the LJ interaction gives rise to a typical phase diagram with a critical point and, at lower temperatures, distinct gas and liquid phases and a triple point, the tWF interaction model

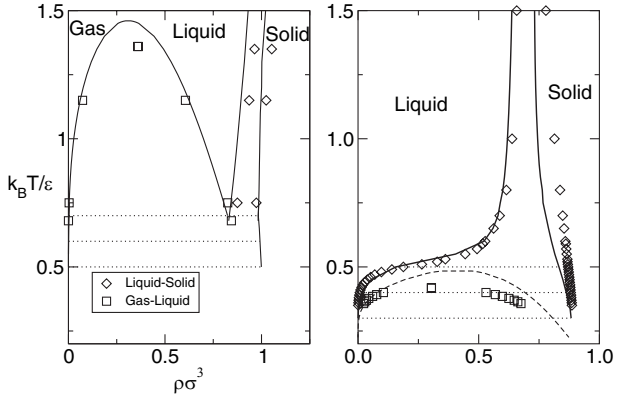

FIG. 1. The phase diagram for a LJ potential (left) and the ten Wolde-Frenkel potential (right). The solid and dashed lines are from the model and the points are from simulation, Refs. [1,23,24], respectively. The dotted lines connect the coexistence points used in Figs. 2 and 3.

gives only a single liquidus phase which is typical of short ranged interactions. Indeed, as the parameter λ in the tWF potential is varied from $\lambda = 1$ to $\lambda = 50$, the phase diagram evolves continuously from one similar to the LJ phase diagram to that shown here possessing a metastable gas-liquid transition [18]. This model is motivated in part by the fact that a dense metastable liquid phase is, in fact, experimentally observed for some proteins. It is this metastable phase which tWF showed to play a role in nucleation of the solid phase from the gas.

Given a reasonable model for the DFT free-energy functional, we now turn to the question of the effect of different paths through density space from a gas of density $\bar{\rho}_{\text{gas}}$ and crystallinity $m_{\text{gas}} = 0$ to a solid with density $\bar{\rho}_{\text{solid}}$ and crystallinity m_{solid}. Here we consider two candidate paths. The first corresponds to a simultaneous densification and ordering of the gas into a solid and is parametrized as

$$\bar{\rho}(x) = \bar{\rho}_{\text{gas}} + x(\bar{\rho}_{\text{solid}} - \bar{\rho}_{\text{gas}}), \qquad m(x) = x m_{\text{solid}}, \quad (4)$$

where $x \in [0, 1]$ is an abstract reaction coordinate. This might be thought of as the ''classical'' path. The second path we consider is a two-step process consisting of first a densification at zero crystallinity followed by an ordering at fixed density

$$\bar{\rho}(x) = [\bar{\rho}_{\text{gas}} + 2x(\bar{\rho}_{\text{solid}} - \bar{\rho}_{\text{gas}})]\Theta(\tfrac{1}{2} - x) + \bar{\rho}_{\text{solid}}\Theta(x - \tfrac{1}{2}),$$
$$m(x) = \Theta(x - \tfrac{1}{2})(2x - 1)m_{\text{solid}}. \quad (5)$$

Figure 2 shows the free-energy landscapes encountered using the tWF potential along both paths for coexisting gas and solid densities at three different temperatures. In all three cases, the classical path requires overcoming a free-energy barrier as expected. The behavior along the nonclassical path is more complex. At the highest temperature, which lies about the critical point of the metastable gas-liquid transition, the nonclassical barrier is somewhat reduced but the effect is not significant. For the intermediate temperature, which is somewhat below the critical point, a second, metastable state appears and the single free-energy barrier splits into two lower barriers. At the lowest temperature, the barriers encountered along the nonclassical path are even lower, so the advantage of this path is even greater. This picture agrees well with that developed by Vekilov and co-workers who have observed, by means of dynamic light scattering, the presence of short-lived dense-liquid droplets in protein solutions [5]. The results for the LJ system, shown in Fig. 3, are unexpected in that a similar phenomenon is observed although the details differ. Again, we show three temperatures, which are this time all below both the critical point and the triple point. The highest temperature is only just below the triple point, and, again, it is clear that the nonclassical path is energetically favored relative to the classical path and that this correlates with the presence of a metastable dense-liquid state. Unlike the previous case, the advantage of passing along the nonclassical path remains more or less constant as the temperature is decreased. Also different is the fact that the barrier between the metastable state and the solid state is much lower than that between the gas and the metastable liquid. This suggests that the droplets in the metastable state will crystallize quickly and will be correspondingly shorter-lived. To check this surprising result, we repeated our calculations using the model described in Refs. [9,17], which is tuned to the LJ potential. While the barriers were somewhat smaller, the qualitative results were the same.

We have presented calculations of the free-energy landscape as a function of density and crystallinity based on a simple, robust free-energy density functional. Our calculations involve no input or parametrization except for the interaction potential. In both cases studied, a model protein and a simple liquid, our results provide direct support for the Ostwald rule of stages for nucleation [19] since the free-energy barriers associated with the metastable intermediate states are lower than those for a direct transition from gas to solid. The results for the model protein interaction agree with the generally accepted picture that crystallization proceeds via a two-step process of densification

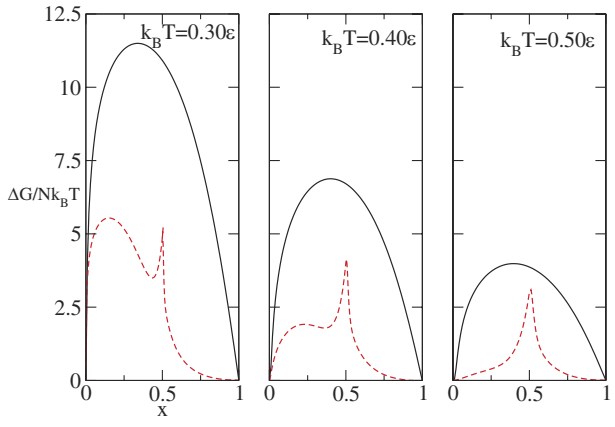

FIG. 2 (color online). The Gibbs free-energy barriers, per atom, for the tWF potential. The solid curve is for the classical path and the broken curve results from densification followed by ordering.

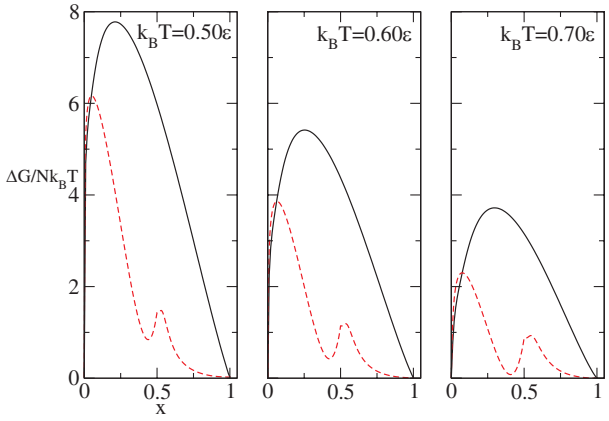

FIG. 3 (color online). Same as Fig. 2 for the LJ potential.

followed by crystallization [4], even when the temperature is slightly above the critical point and no metastable intermediate phase exists. Interestingly, we find similar behavior for simple fluids below the triple point, suggesting that crystallization involving passage through a metastable disordered state may be a generic phenomenon. However, in that case, the metastable state is expected to be shorter-lived compared to the nucleation time, thus making its experimental detection more challenging. The only evidence we are aware of for the two-step nucleation mechanism for nonprotein fluids comes from nonphotochemical laser-induced nucleation of small organic molecules [20,21] and recent molecular dynamics simulations of the crystallization of AgBr from solution [22]. The short lifetime of the metastable phase predicted here would explain why it has not so far been observed experimentally in simple fluids.

For the protein model, our results indicate similar barriers for the gas-liquid and liquid-solid transitions, and it should be noted that the only experimental results indicate that the latter should be much higher than the former [6]. In part, this is because we have presented results for the free-energy landscape for transitions near the coexistence lines. For denser gases, which are supersaturated with respect to crystallization, the free energy of the gas phase moves up so the first barrier is smaller. However, it is important to notice that the crossing of the free-energy barrier is a fundamentally nonequilibrium process, so that kinematics also plays an important role in determining the overall nucleation rates [4,7]. Nevertheless, if crystallization kinetics occurs reasonably close to equilibrium, the free-energy functional will play a central role, since the rates of change of the order parameters will be given by the product of its gradient and of a matrix of phenomenological parameters.

A point which could cause concern is that the paths through parameter space might cross the spinodal and so pass through the two-phase region, where it could be thought that the use of DFT is problematic. In fact, aside from the minima, *all* points on the curves shown in Fig. 2 are thermodynamically unstable. However, the fundamental idea underlying DFT is that any density profile can be stabilized by means of an external field and that the free energies calculated are the intrinsic contribution to the free energy when such a stabilizing field is present (see, e.g., Ref. [12]). Only the intrinsic contribution is used here to estimate the barriers, as the real system must pass through these states without the presence of such a stabilizing field.

One question not answered yet is whether the particular pathways discussed here are the optimal, i.e., minimum energy, pathways. Simple contour plots of the free energy show that the nonclassical paths used here are indeed very close to the optimal paths, as will be discussed at length in a future publication. Another question is the role of surface tension which should, in general, increase the free-energy barriers, as well as the free energies of clusters in the metastable and solid states. Since the penalty due to surface tension is expected to increase as the system passes from the gas to the metastable state to the solid state, we expect that the barriers and the free-energy minima will be shifted accordingly, but it seems unlikely that the overall picture would change, since this would require that the addition of surface tension affect the classical path less than the nonclassical path. A definitive answer to this question will require calculations of free energies for inhomogeneous states, which we are currently pursuing.

It is our pleasure to thank Pieter ten Wolde and Daan Frenkel for making their simulation results available to us. We benefited greatly from discussions with Peter Vekilov and Bruce Garetz. This work was supported in part by the European Space Agency under Contract No. C90105.

[1] P. R. ten Wolde and D. Frenkel, Science **277**, 1975 (1997).
[2] V. Talanquer and D. W. Oxtoby, J. Chem. Phys. **109**, 223 (1998).
[3] A. Shiryayev and J. D. Gunton, J. Chem. Phys. **120**, 8318 (2004).
[4] P. G. Vekilov, Crystal Growth and Design **4**, 671 (2004).
[5] O. Gliko, N. Neumair, W. Pan, I. Haase, M. Fisher, A. Bacher, S. Weinkauf, and P. G. Vekilov, J. Am. Chem. Soc. **127**, 3433 (2005).
[6] L. F. Filobelo, O. Galkin, and P. G. Vekilov, J. Chem. Phys. **123**, 014904 (2005).
[7] G. Nicolis and C. Nicolis, Physica (Amsterdam) **351A**, 22 (2005).
[8] Y. C. Shen and D. W. Oxtoby, Phys. Rev. Lett. **77**, 3585 (1996).
[9] W. A. Curtin and N. W. Ashcroft, Phys. Rev. Lett. **56**, 2775 (1986).
[10] A. Kyrlidis and R. A. Brown, Phys. Rev. E **47**, 427 (1993).
[11] H. C. Andersen, D. Chandler, and J. D. Weeks, Phys. Rev. A **4**, 1597 (1971).
[12] J.-P. Hansen and I. McDonald, *Theory of Simple Liquids* (Academic, San Diego, CA, 1986).
[13] H. S. Kang, C. S. Lee, T. Ree, and F. H. Ree, J. Chem. Phys. **82**, 414 (1985).
[14] Y. Rosenfeld, Phys. Rev. Lett. **63**, 980 (1989).
[15] Y. Rosenfeld, D. Levesque, and J.-J. Weis, J. Chem. Phys. **92**, 6818 (1990).
[16] R. Roth, R. Evans, A. Lang, and G. Kahl, J. Phys. Condens. Matter **14**, 12 063 (2002).
[17] R. Ohnesorge, H. Lowen, and H. Wagner, Phys. Rev. A **43**, 2870 (1991).
[18] J. F. Lutsko and G. Nicolis, J. Chem. Phys. **122**, 244907 (2005).
[19] V. J. Anderson and H. N. W. Lekkerkerker, Nature (London) **416**, 811 (2002).
[20] B. A. Garetz, J. Matic, and A. S. Myerson, Phys. Rev. Lett. **89**, 175501 (2002).
[21] D. W. Oxtoby, Nature (London) **420**, 277 (2002).
[22] J. D. Shore, D. Perchak, and Y. Shnidman, J. Chem. Phys. **113**, 6276 (2000).
[23] L. Verlet and D. Levesque, Physica (Amsterdam) **36**, 254 (1967).
[24] J. P. Hansen and L. Verlet, Phys. Rev. **184**, 151 (1969).